14TH EUROPEAN CONFERENCE ON COMPOSITE MATERIALS
7-10 June 2010, Budapest, Hungary
Paper ID: 684-ECCM14

Buckling, propagation and stability of delaminated anisotropic layers

A. Rhead[1], R. Butler[1*]

[1] *Composites Research Unit, Department of Mechanical Engineering, University of Bath, Claverton Down, Bath, BA2 7AY UK.*
**R.Butler@bath.ac.uk*

Abstract

Previously, the authors have developed a modelling methodology that establishes a threshold strain below which damage propagation will not occur in laminates subject to Compression After Impact (CAI). In order to validate this methodology, a number of quasi-istropic coupons each containing a circular artificial delamination have been tested in axial compression. These coupons had 0^o, $\pm 45^o$ and 90^o dominated thin sublaminates placed above the delamination in order to prove the applicability of the model to sublaminates with high anisotropy. Results indicate the model can predict both the strain at which delaminations in the coupons with 0^o and $\pm 45^o$ dominated sublaminates propagate from their original sites and the stability with which propagation occurred. Analysis of the coupon with a 90^o dominated sublaminate was inconclusive due to an unexpected experimental propagation mode. For all coupons delamination propagation was in the direction of the dominant fibre direction in the sublaminate. The established methodology is shown to be suitable for assessing the damage tolerance of composite laminates.

1. Introduction

Owing to their favourable strength and stiffness properties and the ability to tailor these to give different directional properties carbon fibre reinforced plastics (CFRP) have the potential to radically reduce the weight of any vehicle in which they are employed. However, this weight saving may not have been fully exploited, even in the latest aircraft such as the Boeing 787 and the Airbus A380. There are a number of reasons for this; one of the most significant being Barely Visible Impact Damage (BVID) and the conservative regulations relating to its in service management. When layered structures are impacted delaminations can occur which can severely reduce structural properties, particularly under compressive loads which tend to buckle layers open, creating a mechanism for damage propagation, and premature failure. Consequently, regulations for aircraft manufacture effectively state that, provided the level of impact required to cause BVID is due to a "realistically expected event" (defined as a probability of occurrence of 1 in 10^5 flying hours) it must be assumed that such BVID is present and that the structure must tolerate this damage at ultimate levels of load without failing.

This problem has been the subject of many papers in the composites literature over a period of thirty years. Modelling of the problem has typically been undertaken using FEA, see [1, 2, 3]. However, a few authors have tackled the problem analytically [4, 5, 6] and it is using this approach the method under investigation in this paper was developed. Employing an approach pioneered in [4] the authors have previously derived a simple, semi-numerical, fracture mechanics model to predict critical values of applied stress at which such buckle-driven

propagation of delamination occurs. The model, which makes a number of simplifying assumptions, has been successfully applied to determine stacking sequences that are damage tolerant, and to highlight propagation that is either stable or unstable. In addition the model has been applied successfully to a variety of problems from the literature, see [7, 8, 9].

With the aim of further validating the aforementioned methodology and its simplifying assumptions, this paper presents the results of three experiments on laminates each containing a single artificial circular delamination that produces different types of anisotropy in the thin buckled sublaminate. Three 16-ply quasi-isotropic laminates, denoted 0^o Outer, 45^o Outer and 90^o Outer, each having a single artificial delamination at either the 2nd or 3rd interface were loaded in compression until initial propagation occurred. The three different sublaminates represent different cases of greatest anisotropy i.e. 0^o, $\pm 45^o$ and 90^o dominated sublaminates. The experiments were monitored using a high speed digital image correlation system which produces plots of full field deformation so that the occurrence of critical buckling as well as the onset, mode and stability of propagation could be pin-pointed.

2. Analytical method

A brief derivation of the model, including the key assumptions, equations and concepts, is given here. Full derivations are available elsewhere [7, 8]. The model calculates the threshold strain ε_{th} below which propagation of buckled delaminations will not occur. The model requires the calculation of the buckling strain ε^C of a delaminated circular region for which the composite buckling program VICONOPT [10] is employed (although alternative methods of calculating ε^C would be equally valid). In essence, the delaminated plate is modelled as a thin film such that the plate boundary along the circular perimeter of the delamination is assumed to be clamped. To obtain ε^C, VICONOPT uses the loadings placed on the thin film by axial compression of the full laminate. The program models the plate as a series of finite strips, the edges of which are constrained by nodes approximating a circular boundary. Here, constrained implies that no buckling displacement or rotation is allowed at the nodes, thus approximating a fully clamped boundary. It should be noted that VICONOPT buckling analysis is fully general and can analyse the complex unbalanced and asymmetric sublaminates that can arise in the delaminated sublaminate.

The central concept of the model is to find the difference in energy in the post-buckled sublaminate immediately before and after the growth of a delamination and to compare this difference to the Mode I fracture energy required to create a new unit of delamination. If sufficient energy is available then a new unit of delamination is created and propagation of the delamination will occur. A thin-film assumption is made that has the effect of allowing no energy to be released from the thicker unbuckled portion of the laminate. Prior to and following propagation, the thin buckled region (the thin sublaminate), is considered to contain bending energy and membrane energy which are associated with the diameters l and $l+\delta l$ respectively. Note that l is the diameter of the sublaminate immediately before propagation, and δl is an infinitesimal length associated with the diameter change due to propagation. Energy for propagation is also available in the form of membrane energy released from the section of the sublaminate of length δl which becomes delaminated during propagation. By comparing the difference in energies to G_{IC}, the Strain Energy Release Rate (SERR) required to cause Mode I failure of the resin, it is possible to approximately predict

the threshold strain ε_{th} the strain below which propagation of the delamination produced by the Teflon insert will not occur. This comparison results in the following equation,

$$\varepsilon_{th} = \varepsilon^C \left(\sqrt{4 + \frac{2G_{1C}}{(\varepsilon^C)^2 A_{11}}} - 1 \right) \quad (1)$$

Here, A_{11} is the axial stiffness of the sublaminate. Note that for simplicity, the assumption is made that propagation initiates under Mode I conditions in the direction of applied strain ε. However, propagation transverse to the load is understood to be mixed Mode (the Mode II contribution being particularly large for 90° dominated sublaminates), it is shown in [8] that applying a G_{IC} condition is conservative since less energy needs to be developed in the sublaminate to cause propagation i.e. typically $G_{IIC} > 2G_{IC}$.

In [4] Chai and Babcock show that unstable or stable growth is possible for isotropic and orthotropic sublaminates. Similarly, work in [7] has shown that it is possible to use the model to derive an equation which predicts the stability of propagation. Propagation is stable if,

$$\varepsilon_{th} \geq 3\varepsilon^C \quad (2)$$

3. Experimental method

Three so called quasi-isotropic coupons with equal percentages of 0°, +45°, -45° and 90° plies were made from 0.25mm thick Hexcel M21/T700GC pre-preg layers with material properties E_{11} = 136 GPa, E_{22} = 8.9 GPa, G_{12} = 4.5 GPa, ν_{12} = 0.35 and G_{1C} = 550 J/m^2. Stacking sequences are given in Table 1.

Table 1. Stacking sequences for coupons.

Laminate ID	Lay-up	Thin sublaminate
0° Outer	$[0_2/45/-45/90/45/-45/90]_S$	$[0_2]$
45° Outer	$[45/-45/0_2/-45/90/45/90]_S$	[45/-45]
90° Outer	$[90/0/90/45/-45/45/-45/0]_S$	[90/0/90]

During the manufacturing stage 39mm diameter Teflon circles each having a thickness of 0.0125mm were introduced into the laminates to produce artificial delaminations. Positions of these inserts in relation to coupon boundaries are shown in Fig. 1. Through thickness positions of these artificial delaminations are given in Table 1 by indicating the thin sublaminate created by the delamination. Note that the 90° Outer coupon has a deeper delamination than the other coupons as the model indicated that a $[90_2]$ sublaminate would have a delamination buckling strain that was too high to fail as a consequence of propagation following local delamination buckling. Samples were cured in an LBBC Quicklock Thermoclave using the manufacturer specified curing cycle and subsequently cut into coupons which were tabbed with 1.5mm aluminium plates to provide grip and to prevent crushing at the loading points. Axial compressive load was applied under displacement control at 0.1 mm/min, using an Instron 5585H test machine. An anti-buckling guide with a

circular window 85 mm in diameter was used in order to prevent global buckling. Strains were recorded throughout the tests by two pairs of back-to-back strain gauges attached to a HBM 600 Hz Spider 8 data acquisition system. Gauges 1 and 3 were placed on the face closest to the Teflon insert for all coupons with gauges 4 and 2 placed on the reverse face so as to be back-to-back with 1 and 3, see Fig. 1.

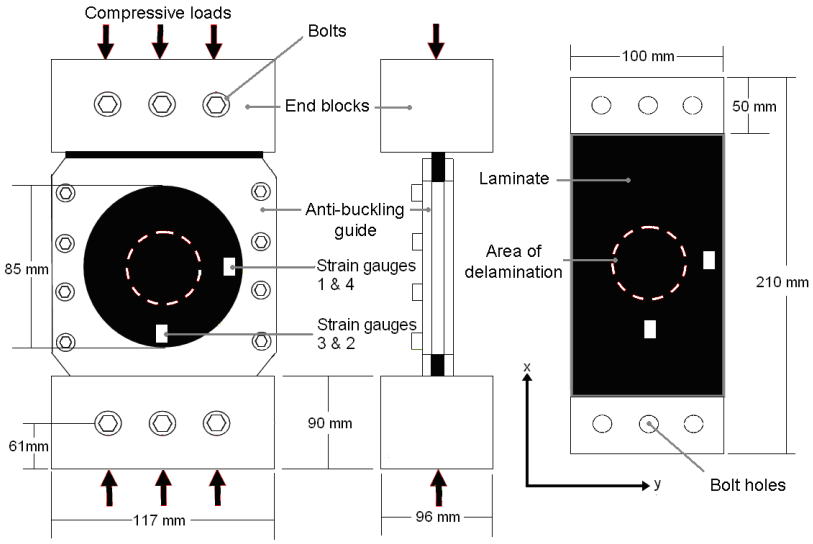

Figure 1. Experimental set-up and coupon details.

The faces of the coupons nearest the Teflon inserts were also covered in a random speckle pattern to allow images and video to be captured of buckling modes and final failure sequences using a Limess VIC-3D HS Digital Image Correlation (DIC) system. This system employs Photron Fastcam SA3 cameras capable of 2000 frames per second (fps) at full resolution. Coupons, end fixtures and anti-buckling guides are described in Fig. 1.

In addition to the above, tests were monitored in real-time using a standard camcorder. An Ultrasonic Sciences C-scan system was used to take C-scans of the coupons prior to testing and following propagation (where possible) to allow the direction and extent of damage growth to be assessed.

4. Results

4.1 0^o Outer laminate

In this test, local buckling occurred at approximately 25kN, seen as a kink on the strain gauge readings in Fig. 2(a). This kinking, not usually associated with a buckling event, was accompanied by an audible click and a spreading of the buckled region, visible on DIC images, to fill the limits of a 39mm circle described by the Teflon insert. From DIC images shown in Fig. 3 it was determined that propagation of the delamination outside the original delaminated area occurred at 65 kN when damage grew in the bottom left corner from the initial site marked by the white circle. This propagation also appears as a kink in the load vs. strain plot in Fig. 2(a). However, subsequent DIC images show steady stable propagation in the 0^o direction until a second major propagation event at 75 kN.

(a)

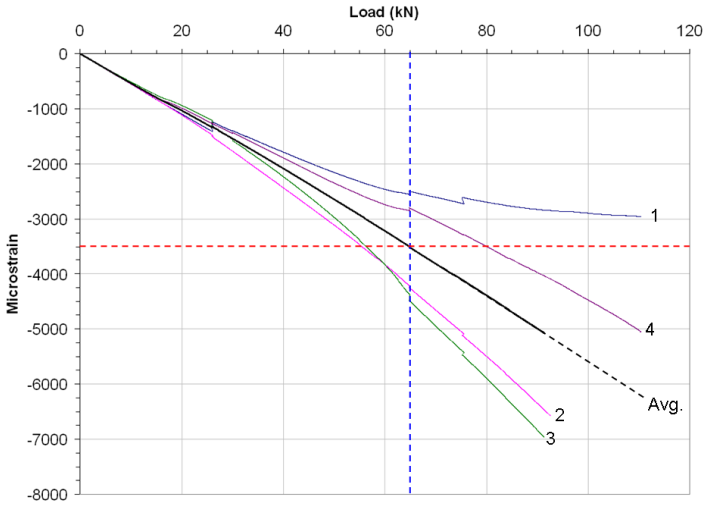

(b)

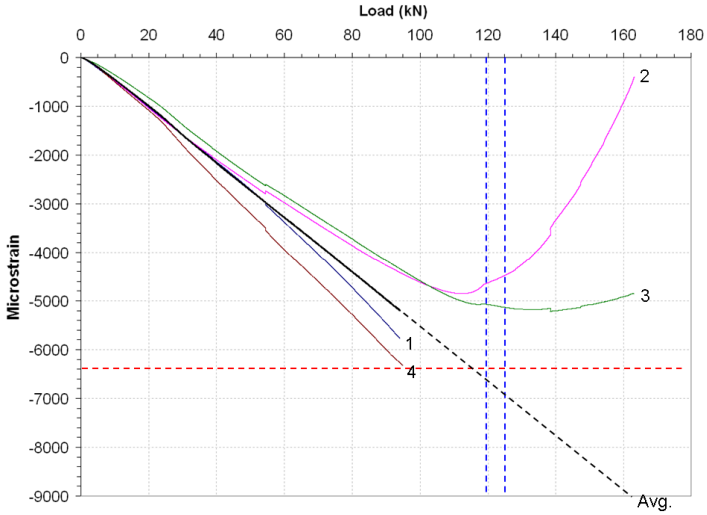

(c)

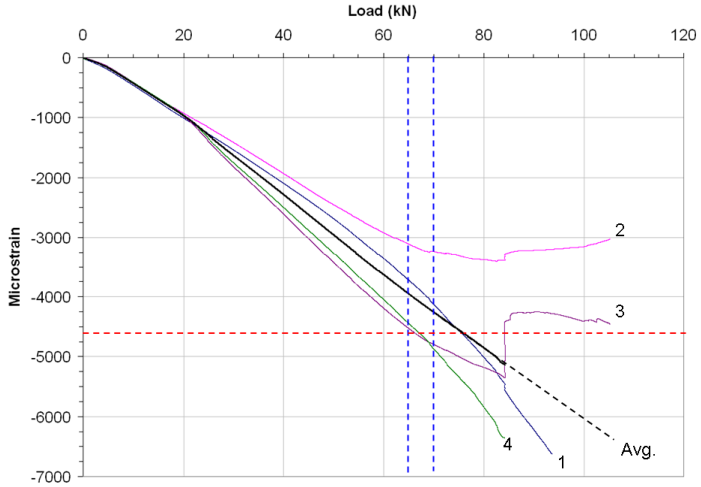

Figure 2. Strain vs. load plots for the (a) 0° Outer, (b) 45° Outer and (c) 90° Outer coupons showing individual strain gauge channels and an average strain which is extended as a dotted line following failure of a strain gauge. Vertical dotted lines indicate bounds of initial propagation established from DIC images. Horizontal dotted lines indicate theoretical propagation predictions.

Note that non-smooth areas in Fig. 3 (and Fig. 4) are a consequence of the system not being able to identify individual speckles due to buckling causing surface deformation leading to areas of intense lighting. Failure occurred at a load of 115 kN, equivalent to a stress of 287.5 MPa. Note gauges 2 and 3 failed at approximately 90-95 kN. Strain gauge readings and DIC images indicate global bending occurred following local buckling and delamination propagation.

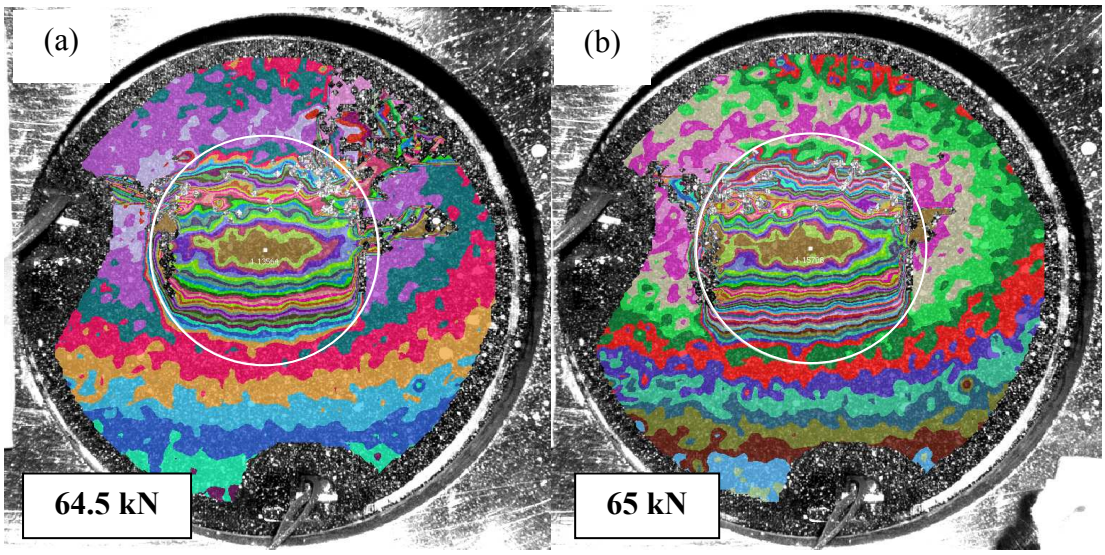

Figure 3. DIC images of the 0° Outer coupon with a 39mm circle highlighting the position of the original delamination showing (a) the buckled non-propagated state at approximately 64.5 kN and (b) the buckled propagated state at 65kN.

4.2 45° Outer laminate

For the 45° Outer laminate, local buckling occurred at approximately 55 kN, seen as a kink on the strain gauge readings in Fig. 2(b).

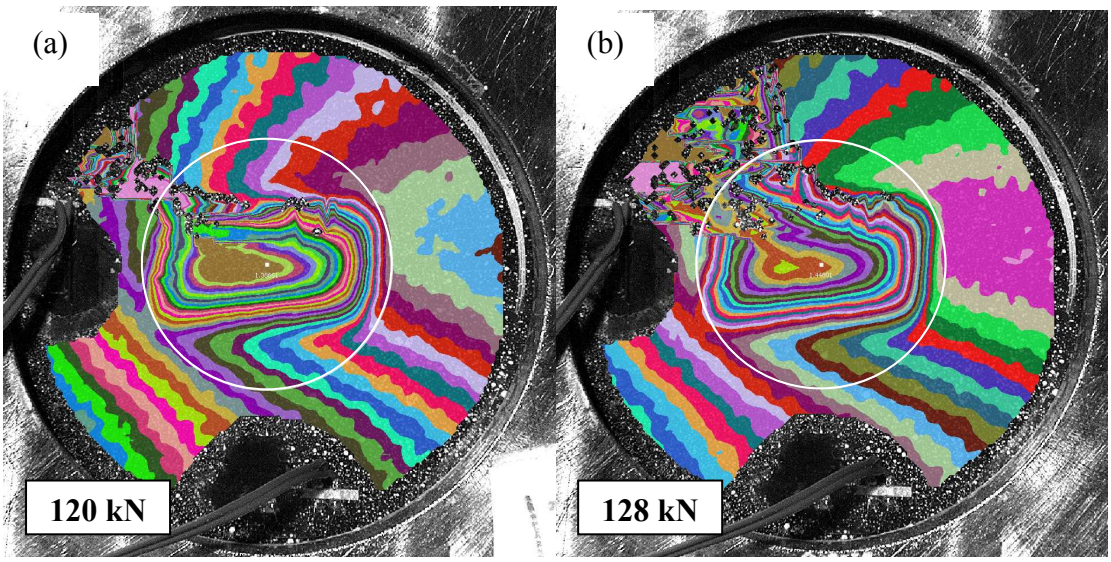

Figure 4. DIC images of the 45° Outer coupon with a 39mm circle highlighting the position of the original delamination showing (a) the buckled non-propagated state at approximately 120 kN and (b) the buckled propagated state at approximately 128kN.

This kinking, as for the 0° Outer coupon, was by an audible click and a spreading of the buckled region, visible on DIC images (see Fig. 4), to fill a section of the 39mm circle described by the Teflon insert. From DIC images shown in Fig. 4. it was determined propagation of the delamination outside the original delaminated area occurred at 120-125 kN when damage grew in the bottom left corner from the initial site marked by the white circle. This propagation appears as a stiffness change (rather than a kink) in the load vs. strain plot in Fig. 2(b) which is consistent with stable propagation. Subsequent DIC images show steady stable propagation in the 45° direction until a second major propagation event at 137 kN which is then followed by further stable propagation until failure. Failure occurred at a load of 162 kN, equivalent to a stress of 405 MPa. Note gauges 1 and 4 failed at approximately 90-95 kN. Strain gauge readings and DIC images indicate the presence of a global bending phenomenon in the latter stages of the test following delamination buckling and propagation.

4.3 90° Outer laminate

In this case, DIC images indicate local buckling initiated at approximately 45 kN and that the buckle was fully formed by 55 kN. Unlike the other two coupons no kink was noted in Fig. 2(c). As can be seen from Fig. 5 the local buckle that formed did not fill the full circle but only a thin elliptical region with major axis in the 90° direction.

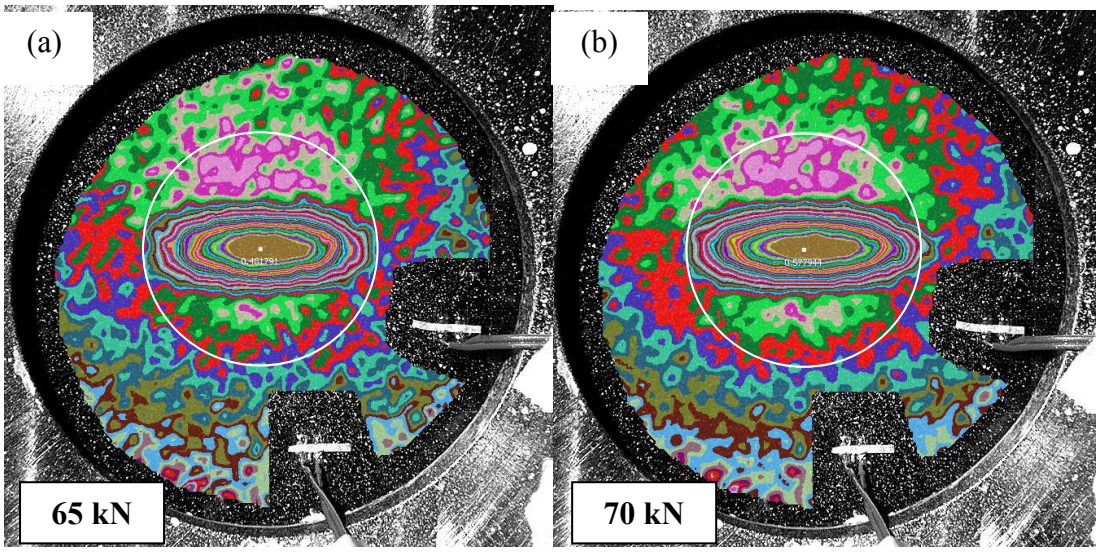

Figure 5. DIC images of the 90° Outer coupon with a 39mm circle highlighting the position of the original delamination showing (a) the buckled non-propagated state at approximately 65 kN and (b) the buckled propagated state at approximately 70 kN.

From DIC images shown in Fig. 5. it was determined that propagation of the delamination outside the original delaminated area occurred at 65-70 kN when damage grew transversely from the initial site marked by the white circle. This propagation appears as a discontinuity or stiffness change depending on the strain gauge channel in the load vs. strain plot in Fig.2(c) which is consistent with stable propagation. Subsequent DIC images show steady propagation in the 90° direction until a second major unstable propagation event at 85 kN which was followed by further rapid propagation until the test was halted to allow C-scan inspection to determine the extent of growth. A C-scan in Fig. 6 taken from the surface nearest to the Teflon insert shows the extent of the damage propagation and also that growth occurred at

both the third interface where the Teflon was sited and the second interface which had no initial delamination. Growth did not spread above the Teflon insert at the 2nd interface.

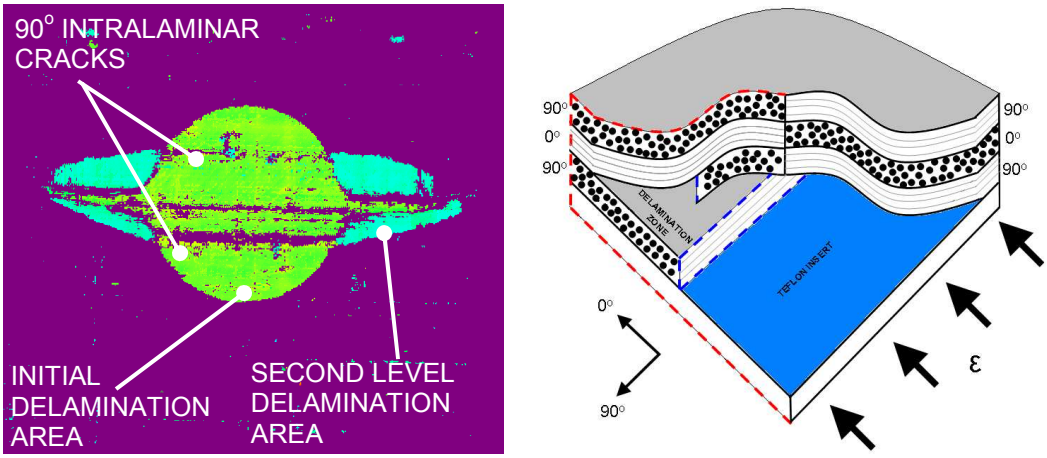

Figure 6. (a) C-scan image of the 90° Outer coupon from the surface closest to the delamination showing the propagated state of damage when the test was halted and the 90° intralaminar splits (b) Schematic of the mode of propagation that produced delaminations at two interfaces.

A second C-scan, not shown here, taken from the opposite side of the coupon showed that delamination growth at the third interface filled approximately the same area as growth at the second. Note gauge 1 failed before the test was stopped at approximately 105 kN. Strain gauge readings, DIC images and load vs. extension plots (not shown here) indicate global bending occurred in prior to initial propagation.

4.4 Comparison with Analytical results

Table 2 gives a summary of the experimental initial propagation results and the analytical predictions of the threshold strains. Table 2 also shows the stability of propagation for each of the 0°, 45° and 90° Outer laminates.

Table 2. Analytical and experimental buckling and propagation strains and theoretical stability values.

Laminate ID	Thin sublaminate	Buckling (μstrain) Analysis / Experiment		Propagation (μstrain) Analysis / Experiment		Stability Eq. (2)
0° Outer	$[0_2]$	682	1250	3551	3544	$\varepsilon_{th} > 3\varepsilon^C$ (Stable)
45° Outer	[45/-45]	807	3005	6512	6700-6800	$\varepsilon_{th} > 3\varepsilon^C$ (Stable)
90° Outer	[90/0/90]	1934	2625-3250	4637*	3945-4260	$\varepsilon_{th} < 3\varepsilon^C$ (Unstable)*

* Note that propagation occurred at two interfaces and the analysis assumes propagation at a single interface.

5. Discussion

Overall divergence in strain gauge readings in Fig. 2 at medium levels of load for the 0°, 45° Outer and 90° Outer (1) coupons is attributed to initial imperfections leading to compression induced bending. Delamination buckling strains were not well predicted by VICONOPT for the 0° and 45° Outer coupons owing to adhesion between the insert and the laminate leading to a delay in local bucking of the delaminated region and an audible click when the buckle was released. However, this was not thought to delay propagation.

Overall growth progression was in the direction of the dominating fibre direction of the buckled sublaminate for all laminates as seen in Figs 3, 4 and 5. Initial propagation was successfully predicted to within 0.2% and 4.4% of the experimental values for the 0^o and 45^o Outer coupons respectively and appeared to be confined to the originally delaminated interface. For these cases the analytical predictions were conservative indicating that the Mode I propagation criteria is a suitable approximation. Although the strain vs. load plot for the 0^o Outer coupon shows a kink at 65kN (Fig 2(a)) and hence unstable propagation, subsequent DIC images show propagation immediately after to be stable indicating an initial dynamic element to the propagation. Figure 2(b) and DIC images showed that delamination in the 45^o Outer coupon was also stable. Global bending/buckling was seen to occur in the 0^o and 45^o Outer specimens but as it followed delamination propagation it will not have invalidated a comparison with analytical predictions; though it may have affected final failure loads.

For the 90^o Outer coupon post-test C-scans, the shape of the buckle and its progression indicated that intraply cracking had occurred parallel to the fibres in the 90^o ply at the bottom of the sublaminate closest to the delamination. The slow formation of the buckle and the lack of a kink in the load vs. strain plot (Fig.2(c)) may also indicate that initial separation of the Teflon from the sublaminate was a result of shear forces. Unusually, delamination growth in the 90^o Outer coupon was not confined to the artificially delaminated 3^{rd} interface but, due to the intraply cracking noted above, spread to the 2^{nd} interface in the sublaminate. Figure 6 demonstrates the mode of growth for the both growth interfaces. At the 2^{nd} interface, due to discontinuities in the 3^{rd} ply caused by the intralaminar crack, peeling (Mode I) forces would be induced by buckling between the 2^{nd} and 3^{rd} plies causing damage to spread in the 0^o direction. Growth would also occur in the 90^o direction at the original delaminated interface where the bottom ply remains connected to the rest of the buckled sublaminate. Hence, due to the complexities of the delamination growth and the unexpected intralaminar crack in the third ply, the theoretical analysis, including growth stability predictions, of the 90^o Outer coupon was considered to be inconclusive and further experiments will be required.

A comparison of growth extent in the 0^o and 90^o Outer coupons, which both had similar initial propagation and failure loads, shows that growth in the 90^o Outer coupon proceeded much further for a given applied load indicating the instability of its growth. The same conclusion can be drawn from a comparison of the 90^o and 45^o Outer coupons. However, note that this implies that the 90^o Outer coupon can withstand a much larger extent of damage than the other coupons without failing. However, for the 90^o Outer coupon, global buckling/bending preceded delamination growth and had an adverse effect on the propagation load of the coupon. This was due to the shape of the global mode which buckled in the opposite direction to the local mode thus increasing local compression of the delamination buckle, see Fig.5.

A comparison of failure loads for the 0^o and 45^o Outer coupons with the load at which the 90^o test was halted under the assumption that this coupon was close to failure (damage had spread to almost the coupons full width) indicates that coupons with 45^o dominated sublaminates are considerably more damage tolerant than those with 0^o or 90^o dominated sublaminates.

6. Conclusions

For all coupons, strain gauge readings, video and DIC observations demonstrate propagation occurred as a result of delamination buckling and was in the principal fibre direction of the delaminated sublaminate.

The model has been validated against two key sublaminates with artificial delaminations that represent two extremes of possible sublaminate construction for laminates made from 0^o and $\pm 45^o$ layers. For these cases comparison of analytical and experimental results in this paper together with those in [7, 8, 9] clearly validate the modelling methodology for calculating delamination propagation thresholds for all laminates with established morphologies and 0^o and 45^o dominated sublaminates. The model is also shown to be capable of making qualitative predictions about overall delamination growth stability.

Overall strengths of coupons indicated that a 45^o sublaminate is preferable to a 0^o sublaminate as its failure load was approximately 50% higher. It is likely that a similar conclusion can be drawn for the 45^o and 90^o Outer coupons as damage in the 90^o Outer coupon had reached the edge of the anti-buckling guide when the test was halted. The 90^o Outer coupon was affected by a global bending/buckling phenomenon and unusual multilayer delamination growth which invalidated its use as a comparison for the analytical model. Hence, the 90^o Outer coupon test should be modified and repeated. In addition, other delamination depths and sublaminate stacking sequences should be investigated together with laminates that have more overall anisotropy than the QI laminates in this paper.

Acknowledgements

The authors would like to thank EPSRC, Airbus UK and GWR for their support and Mr. C. Hurd for his help with manufacturing of coupons.

References

[1] Nilsson K.-F., Asp L.E., Alpman J.E., Nystedt L.: Delamination buckling and growth for delaminations at different depths in a slender composite panel. Int.J. Solids and Structures, **38**, 3039-3071 (2001).
[2] Chen H., Sun X.: Residual compressive strength of laminated plates with delamination. Composite Structures, **47**, 711-717 (1999).
[3] Shen F., Lee K.H., Tay T.E.: Modeling delamination growth in laminated composites. Composites Science and Technology, **61**, 1239-1251 (2001).
[4] Chai H., Babcock C.D., Knauss W.G.: One dimensional modelling of failure in laminated plates by delamination buckling. Int. J. Struct. **7**(11), 1069-1083 (1981).
[5] Kardomateas G.A.: The initial post-buckling and growth behaviour of internal delaminations in composite plates. Journal of Applied Mechanics, **60**, 903-910 (1993).
[6] Flanagan G.: Two-dimensional delamination growth in composite laminates under compression loading. In Composite Materials: Testing and Design. (ed.: Whitcomb JD.) ASTM STP 972. ASTM, Philadelphia, Ch. 8, 180-190 (1988).
[7] Rhead A.T., Butler R., Hunt G.W.: Post-buckled propagation model for compressive fatigue of impact damaged laminates. Int. J. Sol. Struct. **45**(16), 4349-4361 (2008).
[8] Rhead A.T., Butler R.: Compressive static strength model for impact damaged laminates. Compos. Sci. Technol. **69**(14), 2301-2307 (2009).
[9] Rhead A.T., Butler R., Marchant D.: Compressive strength of laminates following free edge impact. Comp. Part A. (2009). doi:10.10.16/j.compositesa.2009.10.024 article in press.
[10] Williams F.W., Kennedy D., Butler R., Anderson M.S.: VICONOPT – Program for exact vibration and buckling analysis or design of prismatic plate assemblies. AIAA, **29**(11), 1927 - 1928 (1991).